

**Updates and discussion:**

[http://www.mitoeagle.org/index.php/MitoEAGLE\\_preprint\\_2018-02-08](http://www.mitoeagle.org/index.php/MitoEAGLE_preprint_2018-02-08)

Correspondence: Gnaiger E

Chair COST Action CA15203 MitoEAGLE – <http://www.mitoeagle.org>

Department of Visceral, Transplant and Thoracic Surgery, D. Swarovski Research  
Laboratory, Medical University of Innsbruck, Innrain 66/4, A-6020 Innsbruck, Austria

Email: [erich.gnaiger@i-med.ac.at](mailto:erich.gnaiger@i-med.ac.at)

Tel: +43 512 566796, Fax: +43 512 566796 20

**Contents****Abstract****Executive summary****1. Introduction** – Box 1: In brief: Mitochondria and Bioblasts**2. Oxidative phosphorylation and coupling states in mitochondrial preparations**

Mitochondrial preparations

*2.1. Respiratory control and coupling*

The steady-state

Specification of biochemical dose

Phosphorylation,  $P_{\mu}$ , and  $P_{\mu}/O_2$  ratio

Control and regulation

Respiratory control and response

Respiratory coupling control and ET-pathway control

Coupling

Uncoupling

*2.2. Coupling states and respiratory rates*

Respiratory capacities in coupling control states

LEAK, OXPHOS, ET, ROX

*2.3. Classical terminology for isolated mitochondria*

States 1–5

**3. Normalization: fluxes and flows***3.1. Normalization: system or sample*

Flow per system,  $I$

Extensive quantities

Size-specific quantities – Box 2: Metabolic fluxes and flows: vectorial and scalar

*3.2. Normalization for system-size: flux per chamber volume*

System-specific flux,  $J_{V,O_2}$

*3.3. Normalization: per sample*

Sample concentration,  $C_{mX}$

Mass-specific flux,  $J_{O_2/mX}$

Number concentration,  $C_{NX}$

Flow per object,  $I_{O_2/X}$

*3.4. Normalization for mitochondrial content*

Mitochondrial concentration,  $C_{mtE}$ , and mitochondrial markers

Mitochondria-specific flux,  $J_{O_2/mtE}$

*3.5. Evaluation of mitochondrial markers**3.6. Conversion: units***4. Conclusions** – Box 3: Mitochondrial and cell respiration**5. References**

102 **Abstract** As the knowledge base and importance of mitochondrial physiology to human health  
103 expand, the necessity for harmonizing nomenclature concerning mitochondrial respiratory  
104 states and rates has become increasingly apparent. Clarity of concept and consistency of  
105 nomenclature are key trademarks of a research field. These trademarks facilitate effective  
106 transdisciplinary communication, education, and ultimately further discovery. Peter Mitchell's  
107 chemiosmotic theory establishes the mechanism of energy transformation and coupling in  
108 oxidative phosphorylation. The unifying concept of the protonmotive force provides the  
109 framework for developing a consistent theory and nomenclature for mitochondrial physiology  
110 and bioenergetics. Herein, we follow IUPAC guidelines on general terms of physical chemistry,  
111 extended by considerations on open systems and irreversible thermodynamics. We align the  
112 nomenclature and symbols of classical bioenergetics with a concept-driven constructive  
113 terminology to express the meaning of each quantity clearly and consistently. In this position  
114 statement, in the frame of COST Action MitoEAGLE, we endeavour to provide a balanced  
115 view on mitochondrial respiratory control and a critical discussion on reporting data of  
116 mitochondrial respiration in terms of metabolic flows and fluxes. Uniform standards for  
117 evaluation of respiratory states and rates will ultimately support the development of databases  
118 of mitochondrial respiratory function in species, tissues, and cells.

119

120 *Keywords:* Mitochondrial respiratory control, coupling control, mitochondrial  
121 preparations, protonmotive force, oxidative phosphorylation, OXPHOS, efficiency, electron  
122 transfer, ET; proton leak, LEAK, residual oxygen consumption, ROX, State 2, State 3, State 4,  
123 normalization, flow, flux, O<sub>2</sub>

124

125

126

---

## 127 Executive summary

128

129 1. In view of <sup>the</sup> broad implications <sup>for</sup> on health care, mitochondrial researchers face an  
130 increasing responsibility to disseminate their fundamental knowledge and novel  
131 discoveries to a wide range of stakeholders and scientists beyond the group of  
132 specialists. This requires implementation of a commonly accepted terminology  
133 within the discipline and standardization in the translational context. Authors,  
134 reviewers, journal editors, and lecturers are challenged to collaborate with the aim  
135 to harmonize the nomenclature in the growing field of mitochondrial physiology  
136 and bioenergetics.

137 2. Aerobic energy metabolism in mammalian mitochondria depends on the coupling of  
138 phosphorylation (ADP → ATP) to O<sub>2</sub> flux in catabolic reactions. In this process of  
139 oxidative phosphorylation, coupling is mediated by translocation of protons  
140 through respiratory proton pumps operating across the inner mitochondrial  
141 membrane and generating or utilizing the protonmotive force measured between  
142 the mitochondrial matrix and intermembrane compartment. Compartmental  
143 coupling thus distinguishes vectorial oxidative phosphorylation from fermentation  
144 as the counterpart of cellular core energy metabolism.

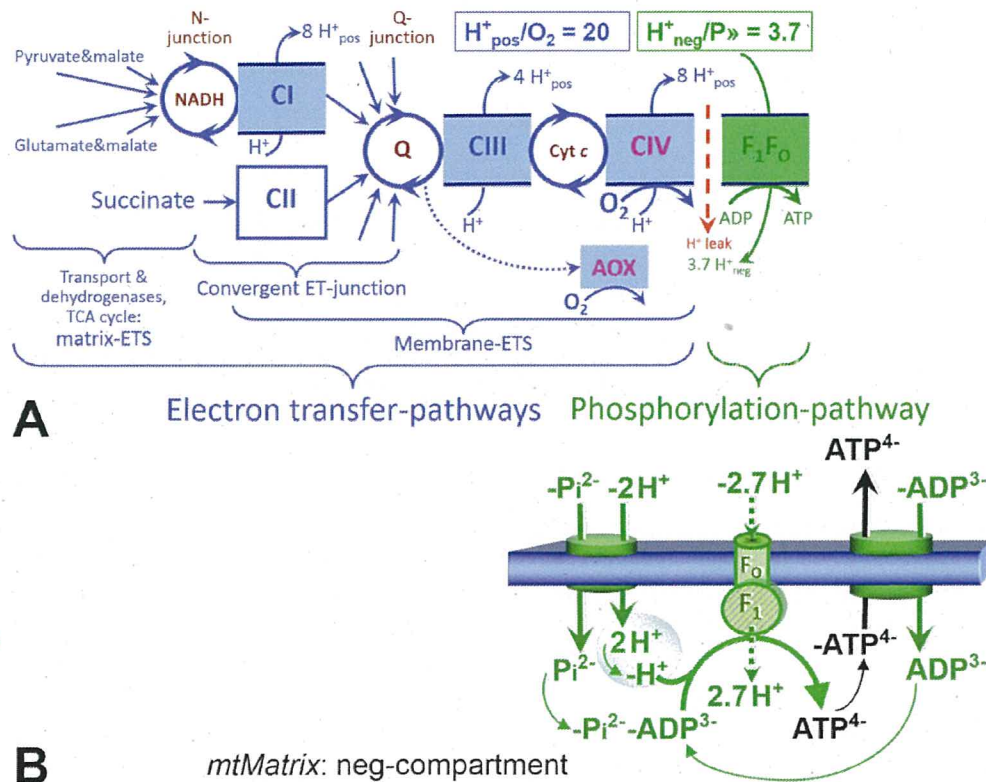
145 3. To exclude fermentation and other cytosolic interactions from exerting an effect on  
146 mitochondrial metabolism, the barrier function of the plasma membrane must be  
147 disrupted. Selective removal or permeabilization of the plasma membrane yields  
148 mitochondrial preparations—including isolated mitochondria, tissue and cellular  
149 preparations—with structural and functional integrity. Then extra-mitochondrial  
150 concentrations of fuel substrates transported into the mitochondrial matrix, ADP,  
151 ATP, inorganic phosphate, and cations including H<sup>+</sup> can be controlled to determine  
152 mitochondrial function under a set of conditions defined as coupling control states.



explicitly

153  
154  
155  
156  
157

A concept-driven terminology of bioenergetics incorporates in its terms and symbols explicitly information on the nature of respiratory states, that makes the technical terms readily recognized and easy to understand.

158  
159  
160  
161  
162  
163  
164  
165  
166  
167  
168  
169  
170  
171  
172  
173  
174  
175  
176  
177  
178  
179

**Fig. 1. The oxidative phosphorylation (OXPHOS) system.** (A) The mitochondrial electron transfer system (ETS) is fuelled by diffusion and transport of substrates across the mtOM and mtIM and consists of the matrix-ETS and membrane-ETS. ET-pathways are coupled to the phosphorylation-pathway. ET-pathways converge at the N-junction and Q-junction. Additional arrows indicate electron entry into the Q-junction through electron transferring flavoprotein, glycerophosphate dehydrogenase, dihydro-orotate dehydrogenase, choline dehydrogenase, and sulfide-ubiquinone oxidoreductase. The dotted arrow indicates the branched pathway of oxygen consumption by alternative quinol oxidase (AOX). The  $H^+_{\text{pos}}/O_2$  ratio is the outward proton flux from the matrix space to the positively (pos) charged compartment, divided by catabolic  $O_2$  flux in the NADH-pathway. The  $H^+_{\text{neg}}/P \gg$  ratio is the inward proton flux from the inter-membrane space to the negatively (neg) charged matrix space, divided by the flux of phosphorylation of ADP to ATP (Eq. 1). These are not fixed stoichiometries due to ion leaks and proton slip. (B) Phosphorylation-pathway catalyzed by the proton pump  $F_1F_0$ -ATPase (F-ATPase, ATP synthase), adenine nucleotide translocase, and inorganic phosphate transporter. The  $H^+_{\text{neg}}/P \gg$  stoichiometry is the sum of the coupling stoichiometry in the F-ATPase reaction ( $-2.7 H^+_{\text{pos}}$  from the positive intermembrane space,  $2.7 H^+_{\text{neg}}$  to the matrix, *i.e.*, the negative compartment) and the proton balance in the translocation of  $ADP^{3-}$ ,  $ATP^{4-}$  and  $P_i^{2-}$ . Modified from (A) Lemieux *et al.* (2017) and (B) Gnaiger (2014).

✓



- 180 4. Mitochondrial coupling states are defined according to the control of respiratory oxygen  
181 flux by the protonmotive force. Capacities of oxidative phosphorylation and  
182 electron transfer capacities are measured at kinetically saturating concentrations of  
183 fuel substrates, ADP and inorganic phosphate, or at optimal uncoupler  
184 concentrations, respectively. Respiratory capacities are a measure of the upper  
185 bound of the rates of respiration, providing reference values for the diagnosis of  
186 health and disease, and for evaluation of the effects of Evolutionary background,  
187 Age, Gender and sex, Lifestyle and Environment (EAGLE).
- 188 5. Some degree of uncoupling is a characteristic of energy-transformations across  
189 membranes. Uncoupling is caused by a variety of physiological, pathological,  
190 toxicological, pharmacological and environmental conditions that exert an  
191 influence not only on the proton leak and cation cycling, but also on proton slip  
192 within the proton pumps and the structural integrity of the mitochondria. A more  
193 loosely coupled state is induced by stimulation of mitochondrial superoxide  
194 formation and the bypass of proton pumps. In addition, uncoupling by application  
195 of protonophores represents an experimental intervention for the transition from a  
196 well-coupled to the noncoupled state of mitochondrial respiration.
- 197 6. Respiratory oxygen consumption rates have to be carefully normalized to enable meta-  
198 analytic studies beyond the specific question of a particular experiment. Therefore,  
199 all raw data should be published in a supplemental table or open access data  
200 repository. Normalization of rates for the volume of the experimental chamber (the  
201 measuring system) is distinguished from normalization for (1) the volume or mass  
202 of the experimental sample, (2) the number of objects (cells, organisms), and (3)  
203 the concentration of mitochondrial markers in the chamber.
- 204 7. The consistent use of terms and symbols discussed in this MitoEAGLE position  
205 statement will facilitate transdisciplinary communication and support further  
206 developments of a database on bioenergetics and mitochondrial physiology. The  
207 present considerations are focused on studies with mitochondrial preparations.  
208 These will be extended in a series of reports on pathway control of mitochondrial  
209 respiration, the protonmotive force, respiratory states in intact cells, and  
210 harmonization of experimental procedures.
- 

#### 215 **Box 1: In brief – Mitochondria and Bioblasts**

216  
217 **Mitochondria** are the oxygen-consuming electrochemical generators evolved from  
218 endosymbiotic bacteria (Margulis 1970; Lane 2005). They were described by Richard Altmann  
219 (1894) as ‘bioblasts’, which include not only the mitochondria as presently defined, but also  
220 symbiotic and free-living bacteria. The word ‘mitochondria’ (Greek mitos: thread; chondros:  
221 granule) was introduced by Carl Benda (1898).

222 Mitochondrial dysfunction is associated with a wide variety of genetic and degenerative  
223 diseases. Robust mitochondrial function is supported by physical exercise and caloric balance,  
224 and is central for sustained metabolic health throughout life. Therefore, a more consistent  
225 presentation of mitochondrial physiology will improve our understanding of the etiology of  
226 disease, the diagnostic repertoire of mitochondrial medicine, with a focus on protective  
227 medicine, lifestyle and healthy aging.

228 We now recognize mitochondria as dynamic organelles with a double membrane that are  
229 contained within eukaryotic cells. The mitochondrial inner membrane (mtIM) shows dynamic  
230 tubular to disk-shaped cristae that separate the mitochondrial matrix, *i.e.*, the negatively charged



231 internal mitochondrial compartment, and the intermembrane space; the latter being positively  
 232 charged and enclosed by the mitochondrial outer membrane (mtOM). The mtIM contains the  
 233 non-bilayer phospholipid cardiolipin, which is not present in any other eukaryotic cellular  
 234 membrane. Cardiolipin promotes the formation of respiratory supercomplexes, which are  
 235 supramolecular assemblies based upon specific, though dynamic, interactions between  
 236 individual respiratory complexes (Greggio *et al.* 2017; Lenaz *et al.* 2017). Membrane fluidity  
 237 exerts an influence on functional properties of proteins incorporated in the membranes  
 238 (Waczulikova *et al.* 2007).

239 Mitochondria are the structural and functional elements of cell respiration. Cell  
 240 respiration is the reduction of oxygen by electron transfer coupled to electrochemical proton  
 241 translocation across the mtIM. In the process of oxidative phosphorylation (OXPHOS), the  
 242 catabolic reaction of oxygen consumption is electrochemically coupled to the transformation of  
 243 energy in the form of adenosine triphosphate (ATP; Mitchell 1961, 2011). Mitochondria are the  
 244 powerhouses of the cell which contain the machinery of the OXPHOS-pathways, including  
 245 transmembrane respiratory complexes—proton pumps with FMN, Fe-S and cytochrome *b*, *c*,  
 246 *aa<sub>3</sub>* redox systems); alternative dehydrogenases and oxidases; the coenzyme ubiquinone (Q);  
 247 F-ATPase or ATP synthase; the enzymes of the tricarboxylic acid cycle and fatty acid oxidation;  
 248 transporters of ions, metabolites and co-factors; and mitochondrial kinases related to energy  
 249 transfer pathways. The mitochondrial proteome comprises over 1,200 proteins (Calvo *et al.*  
 250 2015; 2017), mostly encoded by nuclear DNA (nDNA), with a variety of functions, many of  
 251 which are relatively well known (*e.g.*, apoptosis-regulating proteins), while others are still under  
 252 investigation, or need to be identified (*e.g.*, alanine transporter).

253 There is a constant crosstalk between mitochondria and the other cellular components.  
 254 The crosstalk between mitochondria and endoplasmic reticulum is involved in the regulation of  
 255 calcium homeostasis, cell division, autophagy, differentiation, anti-viral signaling (Murley and  
 256 Nunnari 2016). Cellular mitostasis is maintained through regulation at both the transcriptional  
 257 and post-translational level, through cell signalling including proteostatic (*e.g.*, the ubiquitin-  
 258 proteasome and autophagy-lysosome pathways), and genome stability modules throughout the  
 259 cell cycle or even cell death, contributing to homeostatic regulation in response to varying  
 260 energy demands and stress (Quiros *et al.* 2016). In addition to mitochondrial movement along  
 261 microtubules, mitochondrial morphology can change in response to energy requirements of the  
 262 cell via processes known as fusion and fission, through which mitochondria communicate  
 263 within a network, and in response to intracellular stress factors causing swelling and ultimately  
 264 permeability transition.

265 Mitochondria typically maintain several copies of their own genome known as  
 266 mitochondrial DNA (mtDNA; hundred to thousands per cell; Cummins 1998), which is  
 267 maternally inherited. One exception to strictly maternal inheritance in animals is found in  
 268 bivalves (Breton *et al.* 2007; White *et al.* 2008). mtDNA is 16.5 kB in length, contains 13  
 269 protein-coding genes for subunits of the transmembrane respiratory Complexes CI, CIII, CIV  
 270 and F-ATPase, and also encodes 22 tRNAs and the mitochondrial 16S and 12S rRNA.  
 271 Additional gene content is encoded in the mitochondrial genome, *e.g.*, microRNAs, piRNA,  
 272 smithRNAs, repeat associated RNA, and even additional proteins, *e.g.*, the small peptides  
 273 humanin and MOTS-c (Duarte *et al.* 2014; Lee *et al.* 2015; Cobb *et al.* 2016). The mitochondrial  
 274 genome is regulated and supplemented by nuclear-encoded mitochondrial targeted proteins.

275 Abbreviation: mt, as generally used in mtDNA. Mitochondrion is singular and  
 276 mitochondria is plural.

277 *‘For the physiologist, mitochondria afforded the first opportunity for an experimental*  
 278 *approach to structure-function relationships, in particular those involved in active transport,*  
 279 *vectorial metabolism, and metabolic control mechanisms on a subcellular level’* (Ernster and  
 280 Schatz 1981).

281

---

## 282 1. Introduction

283

284 Mitochondria are the powerhouses of the cell with numerous physiological, molecular,  
285 and genetic functions (**Box 1**). Every study of mitochondrial health and disease is faced with  
286 Evolution, Age, Gender and sex, Lifestyle, and Environment (EAGLE) as essential background  
287 conditions intrinsic to the individual patient or subject, cohort, species, tissue and to some extent  
288 even cell line. As a large and coordinated group of laboratories and researchers, the mission of  
289 the global MitoEAGLE Network is to generate the necessary scale, type, and quality of  
290 consistent data sets and conditions to address this intrinsic complexity. Harmonization of  
291 experimental protocols and implementation of a quality control and data management system  
292 are required to interrelate results gathered across a spectrum of studies and to generate a  
293 rigorously monitored database focused on mitochondrial respiratory function. In this way,  
294 researchers within the same and across different disciplines will be positioned to compare  
295 findings across traditions and generations to an agreed upon set of clearly defined and accepted  
296 international standards.

297 Reliability and comparability of quantitative results depend on the accuracy of  
298 measurements under strictly-defined conditions. A conceptual framework is required to warrant  
299 meaningful interpretation and comparability of experimental outcomes carried out by research  
300 groups at different institutes. With an emphasis on quality of research, collected data can be  
301 useful far beyond the specific question of a particular experiment. Enabling meta-analytic  
302 studies is the most economic way of providing robust answers to biological questions (Cooper  
303 *et al.* 2009). Vague or ambiguous jargon can lead to confusion and may relegate valuable  
304 signals to wasteful noise. For this reason, measured values must be expressed in standard units  
305 for each parameter used to define mitochondrial respiratory function. Harmonization of  
306 nomenclature and definition of technical terms are essential to improve the awareness of the  
307 intricate meaning of current and past scientific vocabulary, for documentation and integration  
308 into databases in general, and quantitative modelling in particular (Beard 2005). The focus on  
309 coupling states and fluxes through metabolic pathways of aerobic energy transformation in  
310 mitochondrial preparations is a first step in the attempt to generate a conceptually-oriented  
311 nomenclature in bioenergetics and mitochondrial physiology. Coupling states of intact cells,  
312 the protonmotive force, and respiratory control by fuel substrates and specific inhibitors of  
313 respiratory enzymes will be reviewed in subsequent communications.

314

315

## 316 2. Oxidative phosphorylation and coupling states in mitochondrial preparations

317 *'Every professional group develops its own technical jargon for talking about matters of*  
318 *critical concern ... People who know a word can share that idea with other members of*  
319 *their group, and a shared vocabulary is part of the glue that holds people together and*  
320 *allows them to create a shared culture'* (Miller 1991).

321

322 **Mitochondrial preparations** are defined as either isolated mitochondria, or tissue and  
323 cellular preparations in which the barrier function of the plasma membrane is disrupted. Since  
324 this entails the loss of cell viability, mitochondrial preparations are not studied *in vivo*. In  
325 contrast to isolated mitochondria and tissue homogenate preparations, mitochondria in  
326 permeabilized tissues and cells are *in situ* relative to the plasma membrane. The plasma  
327 membrane separates the intracellular compartment including the cytosol, nucleus, and  
328 organelles from the environment of the cell. The plasma membrane consists of a lipid bilayer,  
329 embedded proteins, and attached organic molecules that collectively control the selective  
330 permeability of ions, organic molecules, and particles across the cell boundary. The intact  
331 plasma membrane prevents the passage of many water-soluble mitochondrial substrates and  
332 inorganic ions—such as succinate, adenosine diphosphate (ADP) and inorganic phosphate (P<sub>i</sub>),



333 that must be controlled at kinetically-saturating concentrations for the analysis of respiratory  
334 capacities; this limits the scope of investigations into mitochondrial respiratory function in  
335 intact cells.

336 The cholesterol content of the plasma membrane is high compared to mitochondrial  
337 membranes. Therefore, mild detergents—such as digitonin and saponin—can be applied to  
338 selectively permeabilize the plasma membrane by interaction with cholesterol and allow free  
339 exchange of organic molecules and inorganic ions between the cytosol and the immediate cell  
340 environment, while maintaining the integrity and localization of organelles, cytoskeleton, and  
341 the nucleus. Application of optimum concentrations of permeabilization agents (mild detergents  
342 or toxins) leads to washout of cytosolic marker enzymes—such as lactate dehydrogenase—and  
343 results in the complete loss of cell viability, tested by nuclear staining using membrane-  
344 impermeable dyes, while mitochondrial function remains intact. Respiration of isolated  
345 mitochondria remains unaltered after the addition of low concentrations of digitonin or saponin.  
346 In addition to mechanical permeabilization during homogenization of tissue, permeabilization  
347 agents may be applied to ensure permeabilization of all cells. Suspensions of cells  
348 permeabilized in the respiration chamber and crude tissue homogenates contain all components  
349 of the cell at highly dilute concentrations. All mitochondria are retained in chemically-  
350 permeabilized mitochondrial preparations and crude tissue homogenates. In the preparation of  
351 isolated mitochondria, the cells or tissues are homogenized, and the mitochondria are separated  
352 from other cell fractions and purified by differential centrifugation, entailing the loss of a  
353 fraction of the total mitochondrial content. Typical mitochondrial recovery ranges from 30% to  
354 80%. Maximization of the purity of isolated mitochondria may compromise not only the  
355 mitochondrial yield but also the structural and functional integrity. Therefore, protocols to  
356 isolate mitochondria need to be optimized according to each study. The term mitochondrial  
357 preparation does not include further fractionation of mitochondrial components, neither  
358 submitochondrial particles.

359

### 360 2.1. Respiratory control and coupling

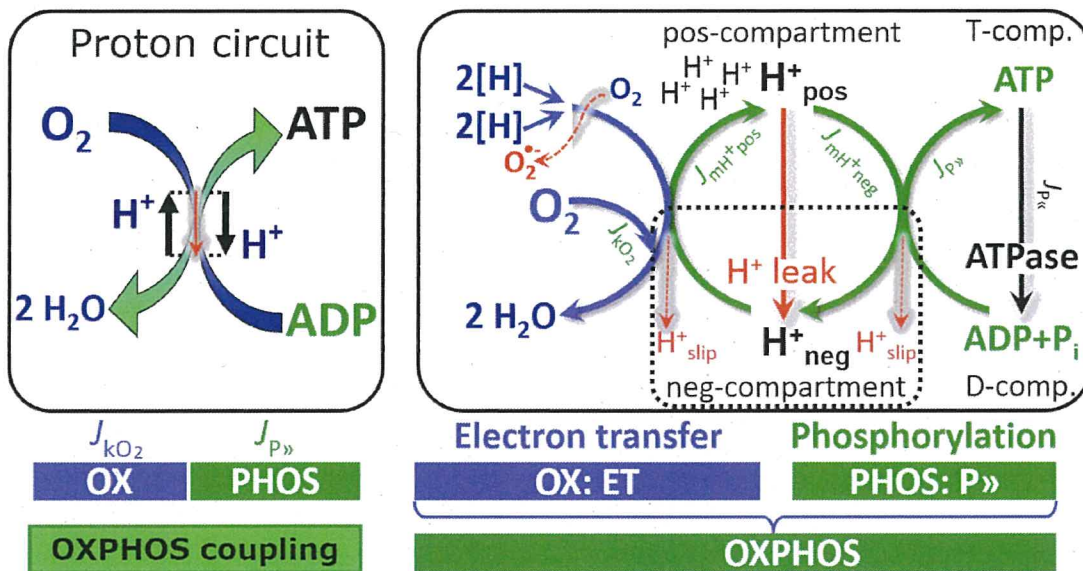
361

362 Respiratory coupling control states are established in studies of mitochondrial  
363 preparations to obtain reference values for various output variables. Physiological conditions *in*  
364 *vivo* deviate from these experimentally obtained states. Since kinetically-saturating  
365 concentrations, *e.g.*, of ADP or oxygen ( $O_2$ ; dioxygen), may not apply to physiological  
366 intracellular conditions, relevant information is obtained in studies of kinetic responses to  
367 variations in  $[ADP]$  or  $[O_2]$  in the range between kinetically-saturating concentrations and  
368 anoxia (Gnaiger 2001).

369 **The steady-state:** Mitochondria represent a thermodynamically open system in non-  
370 equilibrium states of biochemical energy transformation. State variables (protonmotive force;  
371 redox states) and metabolic *rates* (fluxes) are measured in defined mitochondrial respiratory  
372 *states*. Steady-states can be obtained only in open systems, in which changes by *internal*  
373 transformations, *e.g.*,  $O_2$  consumption, are instantaneously compensated for by *external* fluxes,  
374 *e.g.*,  $O_2$  supply, preventing a change of  $O_2$  concentration in the system (Gnaiger 1993b).  
375 Mitochondrial respiratory states monitored in closed systems satisfy the criteria of pseudo-  
376 steady states for limited periods of time, when changes in the system (concentrations of  $O_2$ , fuel  
377 substrates, ADP,  $P_i$ ,  $H^+$ ) do not exert significant effects on metabolic fluxes (respiration,  
378 phosphorylation). Such pseudo-steady states require respiratory media with sufficient buffering  
379 capacity and substrates maintained at kinetically-saturating concentrations, and thus depend on  
380 the kinetics of the processes under investigation.

381 **Specification of biochemical dose:** Substrates, uncouplers, inhibitors, and other  
382 biochemical reagents are titrated to dissect mitochondrial function. Nominal concentrations of  
383 these substances are usually reported as initial amount of substance concentration  $[mol \cdot L^{-1}]$  in

384 the incubation medium. When aiming at the measurement of kinetically saturated processes—  
 385 such as OXPHOS-capacities, the concentrations for substrates can be chosen according to the  
 386 apparent equilibrium constant,  $K_m'$ . In the case of hyperbolic kinetics, only 80% of maximum  
 387 respiratory capacity is obtained at a substrate concentration of four times the  $K_m'$ , whereas  
 388 substrate concentrations of 5, 9, 19 and 49 times the  $K_m'$  are theoretically required for reaching  
 389 83%, 90%, 95% or 98% of the maximal rate (Gnaiger 2001). Other reagents are chosen to  
 390 inhibit or alter some processes. The amount of these chemicals in an experimental incubation  
 391 is selected to maximize effect, avoiding unacceptable off-target consequences that would  
 392 adversely affect the data being sought. Specifying the amount of substance in an incubation as  
 393 nominal concentration in the aqueous incubation medium can be ambiguous (Doskey *et al.*  
 394 2015), particularly for lipophilic substances (oligomycin; uncouplers, permeabilization agents)  
 395 or cations ( $\text{TPP}^+$ ; fluorescent dyes such as safranin, TMRM), which accumulate in biological  
 396 membranes or in the mitochondrial matrix. For example, a dose of digitonin of  $8 \text{ fmol}\cdot\text{cell}^{-1}$  ( $10$   
 397  $\text{pg}\cdot\text{cell}^{-1}$ ;  $10 \mu\text{g}\cdot 10^{-6} \text{ cells}$ ) is optimal for permeabilization of endothelial cells, and the  
 398 concentration in the incubation medium has to be adjusted according to the cell density applied  
 399 (Doerrier *et al.* 2018). Generally, dose/exposure can be specified per unit of biological sample,  
 400 *i.e.*, (nominal moles of xenobiotic)/(number of cells) [ $\text{mol}\cdot\text{cell}^{-1}$ ] or, as appropriate, per mass of  
 401 biological sample [ $\text{mol}\cdot\text{kg}^{-1}$ ]. This approach to specification of dose/exposure provides a  
 402 scalable parameter that can be used to design experiments, help interpret a wide variety of  
 403 experimental results, and provide absolute information that allows researchers worldwide to  
 404 make the most use of published data (Doskey *et al.* 2015).  
 405



406 **Fig. 2. The proton circuit and coupling in oxidative phosphorylation (OXPHOS).**  $2[\text{H}]$   
 407 indicates the reduced hydrogen equivalents of fuel substrates of the catabolic reaction  $k$  with  
 408 oxygen.  $\text{O}_2$  flux,  $J_{\text{kO}_2}$ , through the catabolic ET-pathway, is coupled to flux through the  
 409 phosphorylation-pathway of  $\text{ADP}$  to  $\text{ATP}$ ,  $J_{\text{P}}$ . The proton pumps of the ET-pathway drive  
 410 proton flux into the positive (pos) compartment,  $J_{\text{mH}^+\text{pos}}$ , generating the output protonmotive  
 411 force (motive, subscript  $m$ ). F-ATPase is coupled to inward proton current into the negative  
 412 (neg) compartment,  $J_{\text{mH}^+\text{neg}}$ , to phosphorylate  $\text{ADP} + \text{P}_i$  to  $\text{ATP}$ . The system defined by the  
 413 boundaries (full black line) is not a black box, but is analysed as a compartmental system. The  
 414 negative compartment (neg-compartment, enclosed by the dotted line) is the matrix space,  
 415 separated by the mtIM from the positive compartment (pos-compartment).  $\text{ADP} + \text{P}_i$  and  $\text{ATP}$   
 416 are the substrate- and product-compartments (scalar  $\text{ADP}$  and  $\text{ATP}$  compartments, D-comp.  
 417 and T-comp.), respectively. At steady-state proton turnover,  $J_{\infty\text{H}^+}$ , and  $\text{ATP}$  turnover,  $J_{\infty\text{P}}$ ,  
 418



419 maintain concentrations constant, when  $J_{mH+\infty} = J_{mH+pos} = J_{mH+neg}$ , and  $J_{P\infty} = J_{P\gg} = J_{P\ll}$ . Modified  
420 from Gnaiger (2014).

421 **Phosphorylation, P $\gg$ , and P $\gg$ /O $_2$  ratio:** *Phosphorylation* in the context of OXPHOS is  
422 defined as phosphorylation of ADP by P $_i$  to ATP. On the other hand, the term phosphorylation  
423 is used generally in many contexts, *e.g.*, protein phosphorylation. This justifies consideration  
424 of a symbol more discriminating and specific than P as used in the P/O ratio (phosphate to  
425 atomic oxygen ratio), where P indicates phosphorylation of ADP to ATP or GDP to GTP. We  
426 propose the symbol P $\gg$  for the endergonic (uphill) direction of phosphorylation ADP $\rightarrow$ ATP,  
427 and likewise the symbol P $\ll$  for the corresponding exergonic (downhill) hydrolysis ATP $\rightarrow$ ADP  
428 (Fig. 2). P $\gg$  refers mainly to electrontransfer phosphorylation but may also involve substrate-  
429 level phosphorylation as part of the tricarboxylic acid (TCA) cycle (succinyl-CoA ligase) and  
430 phosphorylation of ADP catalyzed by phosphoenolpyruvate carboxykinase.  
431 Transphosphorylation is performed by adenylate kinase, creatine kinase, hexokinase and  
432 nucleoside diphosphate kinase. In isolated mammalian mitochondria, ATP production  
433 catalyzed by adenylate kinase (2 ADP  $\leftrightarrow$  ATP + AMP) proceeds without fuel substrates in the  
434 presence of ADP (Komlódi and Tretter 2017). Kinase cycles are involved in intracellular energy  
435 transfer and signal transduction for regulation of energy flux.

436 The P $\gg$ /O $_2$  ratio (P $\gg$ /4 e $^-$ ) is two times the 'P/O' ratio (P $\gg$ /2 e $^-$ ) of classical bioenergetics.  
437 P $\gg$ /O $_2$  is a generalized symbol, independent phosphorylation assessment by determination of P $_i$   
438 consumption (P $_i$ /O $_2$  flux ratio), ADP depletion (ADP/O $_2$  flux ratio), or ATP production  
439 (ATP/O $_2$  flux ratio). The mechanistic P $\gg$ /O $_2$  ratio—or P $\gg$ /O $_2$  stoichiometry—is calculated from  
440 the proton-to-O $_2$  and proton-to-phosphorylation coupling stoichiometries (Fig. 1A),  
441

441

$$442 \quad P\gg/O_2 = \frac{H_{pos}^+/O_2}{H_{neg}^+/P\gg} \quad (1)$$

443

444 The H $^+_{pos}$ /O $_2$  *coupling stoichiometry* (referring to the full 4 electron reduction of O $_2$ ) depends  
445 on the ET-pathway control state, *which* defines the relative involvement of the three coupling  
446 sites (CI, CIII and CIV) in the catabolic pathway of electrons to O $_2$ . This varies with: (1) a  
447 bypass of CI by single or multiple electron input into the Q-junction; and (2) a bypass of CIV  
448 by involvement of AOX. H $^+_{pos}$ /O $_2$  is 12 in the ET-pathways involving CIII and CIV as proton  
449 pumps, increasing to 20 for the NADH-pathway (Fig. 1A), but a general consensus on H $^+_{pos}$ /O $_2$   
450 stoichiometries remains to be reached (Hinkle 2005; Wikström and Hummer 2012; Sazanov  
451 2015). The H $^+_{neg}$ /P $\gg$  coupling stoichiometry (3.7; Fig. 1A) is the sum of 2.7 H $^+_{neg}$  required by  
452 the F-ATPase of vertebrate and most invertebrate species (Watt *et al.* 2010) and the proton  
453 balance in the translocation of ADP, ATP and P $_i$  (Fig. 1B). Taken together, the mechanistic  
454 P $\gg$ /O $_2$  ratio is calculated at 5.4 and 3.3 for NADH- and succinate-linked respiration, respectively  
455 (Eq. 1). The corresponding classical P $\gg$ /O ratios (referring to the 2 electron reduction of 0.5 O $_2$ )  
456 are 2.7 and 1.6 (Watt *et al.* 2010), in agreement with the measured P $\gg$ /O ratio for succinate of  
457  $1.58 \pm 0.02$  (Gnaiger *et al.* 2000).

458 The effective P $\gg$ /O $_2$  flux ratio ( $Y_{P\gg/O_2} = J_{P\gg}/J_{kO_2}$ ) is diminished relative to the mechanistic  
459 P $\gg$ /O $_2$  ratio by intrinsic and extrinsic uncoupling and dyscoupling (Fig. 3). Such generalized  
460 uncoupling is different from switching to mitochondrial pathways that involve fewer than three  
461 proton pumps ('coupling sites': Complexes CI, CIII and CIV), bypassing CI through multiple  
462 electron entries into the Q-junction, or CIII and CIV through AOX (Fig. 1). Reprogramming of  
463 mitochondrial pathways may be considered as a switch of gears (changing the stoichiometry)  
464 rather than uncoupling (loosening the stoichiometry). In addition,  $Y_{P\gg/O_2}$  depends on several  
465 experimental conditions of flux control, increasing as a hyperbolic function of [ADP] to a  
466 maximum value (Gnaiger 2001).

467 **Control and regulation:** The terms metabolic *control* and *regulation* are frequently used  
468 synonymously, but are distinguished in metabolic control analysis: 'We could understand the



469 regulation as the mechanism that occurs when a system maintains some variable constant over  
 470 time, in spite of fluctuations in external conditions (homeostasis of the internal state). On the  
 471 other hand, metabolic control is the power to change the state of the metabolism in response to  
 472 an external signal' (Fell 1997). Respiratory control may be induced by experimental control  
 473 signals that *exert* an influence on: (1) ATP demand and ADP phosphorylation-rate; (2) fuel  
 474 substrate composition, pathway competition; (3) available amounts of substrates and O<sub>2</sub>, *e.g.*,  
 475 starvation and hypoxia; (4) the protonmotive force, redox states, flux–force relationships,  
 476 coupling and efficiency; (5) Ca<sup>2+</sup> and other ions including H<sup>+</sup>; (6) inhibitors, *e.g.*, nitric oxide  
 477 or intermediary metabolites such as oxaloacetate; (7) signalling pathways and regulatory  
 478 proteins, *e.g.*, insulin resistance, transcription factor hypoxia inducible factor 1. *Mechanisms* of  
 479 respiratory control and regulation include adjustments of: (1) enzyme activities by allosteric  
 480 mechanisms and phosphorylation; (2) enzyme content, concentrations of cofactors and  
 481 conserved moieties—such as adenylates, nicotinamide adenine dinucleotide [NAD<sup>+</sup>/NADH],  
 482 coenzyme Q, cytochrome *c*); (3) metabolic channeling by supercomplexes; and (4)  
 483 mitochondrial density (enzyme concentrations and membrane area) and morphology (cristae  
 484 folding, fission and fusion). Mitochondria are targeted directly by hormones, thereby affecting  
 485 their energy metabolism (Lee *et al.* 2013; Gerö and Szabo 2016; Price and Dai 2016; Moreno  
 486 *et al.* 2017). Evolutionary or acquired differences in the genetic and epigenetic basis of  
 487 mitochondrial function (or dysfunction) between subjects and gene therapy; age; gender,  
 488 biological sex, and hormone concentrations; life style including exercise and nutrition; and  
 489 environmental issues including thermal, atmospheric, toxicological and pharmacological  
 490 factors, exert an influence on all control mechanisms listed above. For reviews, see Brown  
 491 1992; Gnaiger 1993a, 2009; 2014; Paradies *et al.* 2014; Morrow *et al.* 2017.

492 **Respiratory control and response:** Lack of control by a metabolic pathway, *e.g.*,  
 493 phosphorylation-pathway, means that there will be no response to a variable activating it, *e.g.*,  
 494 [ADP]. The reverse, however, is not true as the absence of a response to [ADP] does not exclude  
 495 the phosphorylation-pathway from having some degree of control. The degree of control of a  
 496 component of the OXPHOS-pathway on an output variable—such as O<sub>2</sub> flux, will in general  
 497 be different from the degree of control on other outputs—such as phosphorylation-flux or  
 498 proton leak flux. Therefore, it is necessary to be specific as to which input and output are under  
 499 consideration (Fell 1997).

500 **Respiratory coupling control and ET-pathway control:** Respiratory control refers to  
 501 the ability of mitochondria to adjust O<sub>2</sub> flux in response to external control signals by engaging  
 502 various mechanisms of control and regulation. Respiratory control is monitored in a  
 503 mitochondrial preparation under conditions defined as respiratory states. When  
 504 phosphorylation of ADP to ATP is stimulated or depressed, an increase or decrease is observed  
 505 in electron flux linked to O<sub>2</sub> flux in respiratory coupling states of intact mitochondria  
 506 ('controlled states' in the classical terminology of bioenergetics). Alternatively, coupling of  
 507 electron transfer with phosphorylation is disengaged by disruption of the integrity of the mtIM  
 508 or by uncouplers, functioning like a clutch in a mechanical system. The corresponding coupling  
 509 control state is characterized by high levels of O<sub>2</sub> consumption without control by P»  
 510 ('uncontrolled state').

511 ET-pathway control states are obtained in mitochondrial preparations by depletion of  
 512 endogenous substrates and addition to the mitochondrial respiration medium of fuel substrates  
 513 (CHNO; 2[H] in **Fig. 2**) and specific inhibitors, activating selected mitochondrial catabolic  
 514 pathways, *k* (**Fig. 1**). Coupling control states and pathway control states are complementary,  
 515 since mitochondrial preparations depend on an exogenous supply of pathway-specific fuel  
 516 substrates and oxygen (Gnaiger 2014).

517 **Coupling:** In mitochondrial electron transfer (**Fig. 1**), vectorial transmembrane proton  
 518 flux is coupled through the proton pumps CI, CIII and CIV to the catabolic flux of scalar  
 519 reactions, collectively measured as O<sub>2</sub> flux (**Fig. 2**). Thus mitochondria are elements of energy



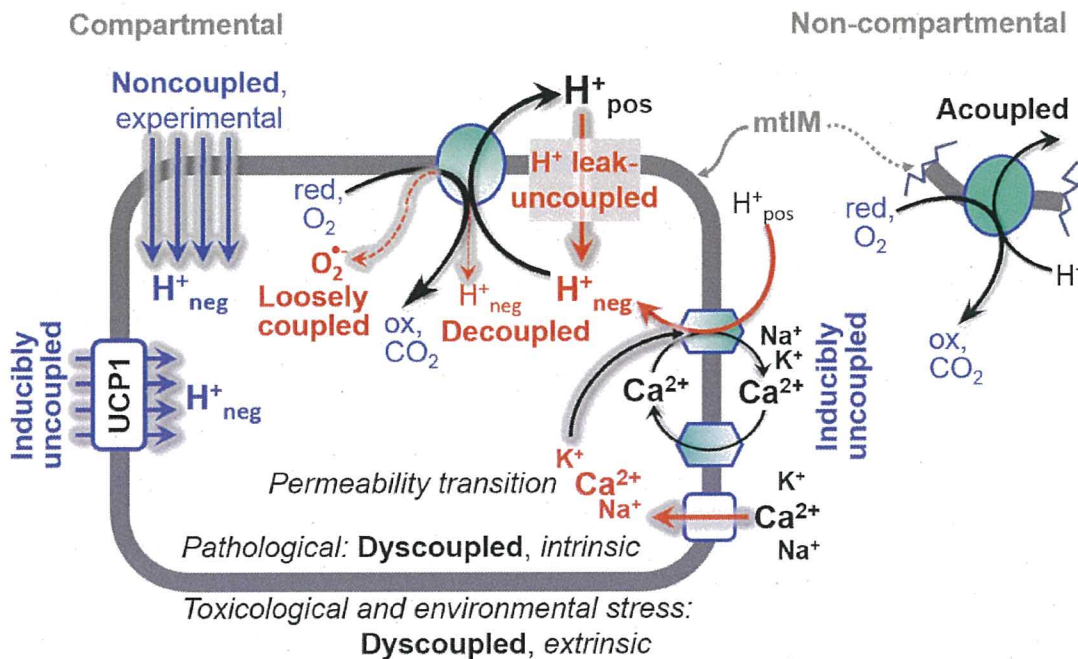
*is a conserved quantity and*

520 transformation. Energy cannot be lost or produced in any internal process (First Law of  
521 thermodynamics). Open and closed systems can gain or lose energy only by external fluxes—  
522 by exchange with the environment. Energy is a conserved quantity. Therefore, energy can  
523 neither be produced by mitochondria, nor is there any internal process without energy  
524 conservation. Exergy is defined as the 'free energy' with the potential to perform work.  
525 *Coupling* is the mechanistic linkage of an exergonic process (spontaneous, negative exergy  
526 change) with an endergonic process (positive exergy change) in energy transformations which  
527 conserve part of the exergy that would be irreversible lost or dissipated in an uncoupled process.

528 **Uncoupling:** Uncoupling of mitochondrial respiration is a general term comprising  
529 diverse mechanisms. Differences of terms—uncoupled vs. noncoupled—are easily overlooked,  
530 although they relate to different mechanisms of uncoupling (**Fig. 3**).

- 531 1. Proton leak across the mtIM from the pos- to the neg-compartment (**Fig. 2**);
- 532 2. Cycling of other cations, strongly stimulated by permeability transition;
- 533 3. Proton slip in the proton pumps when protons are effectively not pumped (CI, CIII and  
534 CIV) or are not driving phosphorylation (F-ATPase);
- 535 4. Loss of compartmental integrity when electron transfer is uncoupled;
- 536 5. Electron leak in the loosely coupled univalent reduction of  $O_2$  to superoxide ( $O_2^{\cdot-}$ ;  
537 superoxide anion radical).

538



539

540 **Fig 3. Mechanisms of respiratory uncoupling.** An intact mitochondrial inner membrane,  
541 mtIM, is required for vectorial, compartmental coupling. 'Acoupled' respiration is the  
542 consequence of structural disruption with catalytic activity of non-compartmental  
543 mitochondrial fragments. Inducibly uncoupled (activation of UCP1) and experimentally  
544 noncoupled respiration (titration of protonophores) stimulate respiration to maximum  $O_2$  flux.  
545  $H^+$  leak-uncoupled, decoupled, and loosely coupled respiration are components of intrinsic  
546 uncoupling. Pathological dysfunction may affect all types of uncoupling, including  
547 permeability transition, causing intrinsically dyscoupled respiration. Similarly, toxicological  
548 and environmental stress factors can cause extrinsically dyscoupled respiration.

549

550 2.2. Coupling states and respiratory rates

551

552 **Respiratory capacities in coupling control states:** To extend the classical nomenclature  
 553 on mitochondrial coupling states (Section 2.3) by a concept-driven terminology that  
 554 incorporates explicitly information on the nature of respiratory states, the terminology must be  
 555 general and not restricted to any particular experimental protocol or mitochondrial preparation  
 556 (Gnaiger 2009). We focus primarily on the conceptual ‘why’, along with clarification of the  
 557 experimental ‘how’. Respiratory capacities delineate, comparable to channel capacity in  
 558 information theory (Schneider 2006), the upper bound of the rate of respiration measured in  
 559 defined coupling control states and electron transfer-pathway (ET-pathway) states (Fig. 4).

560

561 **Fig. 4. Four-compartment model of oxidative phosphorylation.** Respiratory states (ET, OXPHOS, LEAK;

562 **Table 1**) and corresponding rates ( $E$ ,  $P$ ,  $L$ ) are connected by the protonmotive force,  $\Delta p$ . ET-capacity,  $E$ , is partitioned into (1) dissipative LEAK-respiration,  $L$ , when the Gibbs energy change of catabolic  $O_2$  flux is irreversibly

572 lost, (2) net OXPHOS-capacity,  $P-L$ , with partial conservation of the capacity to perform work, and (3) the excess capacity,  $E-P$ . Modified from Gnaiger (2014).

574

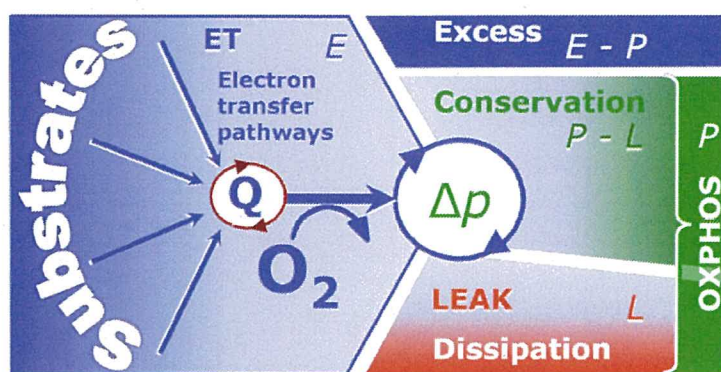
575 **Table 1. Coupling states and residual oxygen consumption in mitochondrial preparations in relation to respiration- and phosphorylation-flux,  $J_{kO_2}$  and  $J_{P_{\gg}}$ , and protonmotive force,  $\Delta p$ .** Coupling states are established at kinetically-saturating concentrations of fuel substrates and  $O_2$ .

578

State	$J_{kO_2}$	$J_{P_{\gg}}$	$\Delta p$	Inducing factors	Limiting factors
LEAK	$L$ ; low, cation leak-dependent respiration	0	max.	proton leak, slip, and cation cycling	$J_{P_{\gg}} = 0$ : (1) without ADP, $L_N$ ; (2) max. ATP/ADP ratio, $L_T$ ; or (3) inhibition of the phosphorylation-pathway, $L_{Omy}$
OXPHOS	$P$ ; high, ADP-stimulated respiration	max.	high	kinetically-saturating [ADP] and $[P_i]$	$J_{P_{\gg}}$ by phosphorylation-pathway; or $J_{kO_2}$ by ET-capacity
ET	$E$ ; max., noncoupled respiration	0	low	optimal external uncoupler concentration for max. $J_{O_2, E}$	$J_{kO_2}$ by ET-capacity
ROX	$R_{ox}$ ; min., residual $O_2$ consumption	0	0	$J_{O_2, Rox}$ in non-ET-pathway oxidation reactions	full inhibition of ET-pathway; or absence of fuel substrates

579

580 To provide a diagnostic reference for respiratory capacities of core energy metabolism,  
 581 the capacity of oxidative phosphorylation, OXPHOS, is measured at kinetically-saturating  
 582 concentrations of ADP and  $P_i$ . The oxidative ET-capacity reveals the limitation of OXPHOS-





583 capacity mediated by the *phosphorylation*-pathway. The ET- and phosphorylation-pathways  
 584 comprise coupled segments of the OXPHOS-system. ET-capacity is measured as noncoupled  
 585 respiration by application of *external uncouplers*. The contribution of *intrinsically uncoupled*  
 586 O<sub>2</sub> consumption is studied in the absence of ADP—by not stimulating phosphorylation, or by  
 587 inhibition of the phosphorylation-pathway. The corresponding states are collectively classified  
 588 as LEAK-states, when O<sub>2</sub> consumption compensates mainly for ion leaks, including the proton  
 589 leak. Defined coupling states are induced by: (1) adding cation chelators such as EGTA, binding  
 590 free Ca<sup>2+</sup> and thus limiting cation cycling; (2) adding ADP and P<sub>i</sub>; (3) inhibiting the  
 591 phosphorylation-pathway; and (4) uncoupler titrations, while maintaining a defined ET-  
 592 pathway state with constant fuel substrates and inhibitors of specific branches of the ET-  
 593 pathway (**Fig. 1**).

594 The three coupling states, ET, LEAK and OXPHOS, are shown schematically with the  
 595 corresponding respiratory rates, abbreviated as *E*, *L* and *P*, respectively (**Fig. 4**). We distinguish  
 596 metabolic *pathways* from metabolic *states* and the corresponding metabolic *rates*; for example:  
 597 ET-pathways (**Fig. 4**), ET-state (**Fig. 5C**), and ET-capacity, *E*, respectively (**Table 1**). The  
 598 protonmotive force is *high* in the OXPHOS-state when it drives phosphorylation, *maximum* in  
 599 the LEAK-state of coupled mitochondria, driven by LEAK-respiration at a minimum back flux  
 600 of cations to the matrix side, and *very low* in the ET-state when uncouplers short-circuit the  
 601 proton cycle (**Table 1**).

602 *E* may exceed or be equal to *P*.  $E > P$  is observed in many types of mitochondria, varying  
 603 between species, tissues and cell types (Gnaiger 2009).  $E - P$  is the excess ET-capacity pushing  
 604 the phosphorylation-flux (**Fig. 1B**) to the limit of its *capacity of utilizing* the protonmotive force.  
 605 In addition, the magnitude of  $E - P$  depends on the tightness of respiratory coupling or degree of  
 606 uncoupling, since an increase of *L* causes *P* to increase towards the limit of *E*. The *excess E-P*  
 607 capacity,  $E - P$ , therefore, provides a sensitive diagnostic indicator of specific injuries of the  
 608 phosphorylation-pathway, under conditions when *E* remains constant but *P* declines relative to  
 609 controls (**Fig. 4**). Substrate cocktails supporting simultaneous convergent electron transfer to  
 610 the Q-junction for reconstitution of TCA cycle function establish pathway control states with  
 611 high ET-capacity, and consequently increase the sensitivity of the  $E - P$  assay.

612 *E* cannot theoretically be lower than *P*.  $E < P$  must be discounted as an artefact, which  
 613 may be caused experimentally by: (1) loss of oxidative capacity during the time course of the  
 614 respirometric assay, since *E* is measured subsequently to *P*; (2) using insufficient uncoupler  
 615 concentrations; (3) using high uncoupler concentrations which inhibit ET (Gnaiger 2008); (4)  
 616 high oligomycin concentrations applied for measurement of *L* before titrations of uncoupler,  
 617 when oligomycin exerts an inhibitory effect on *E*. On the other hand, the excess ET-capacity is  
 618 overestimated if non-saturating [ADP] or [P<sub>i</sub>] are used. See State 3 in the next section.

619 The net OXPHOS-capacity is calculated by subtracting *L* from *P* (**Fig. 4**). Then the net  
 620  $P \gg O_2$  equals  $P \gg (P - L)$ , wherein the dissipative LEAK component in the OXPHOS-state may  
 621 be overestimated. This can be avoided by measuring LEAK-respiration in a state when the  
 622 protonmotive force is adjusted to its slightly lower value in the OXPHOS-state—by titration of  
 623 an ET inhibitor (Divakaruni and Brand 2011). Any turnover-dependent components of proton  
 624 leak and slip, however, are underestimated under these conditions (Garlid *et al.* 1993). In  
 625 general, it is inappropriate to use the term *ATP production* or *ATP turnover* for the difference  
 626 of O<sub>2</sub> flux measured in states *P* and *L*. The difference  $P - L$  is the upper limit of the part of  
 627 OXPHOS-capacity that is freely available for ATP production (corrected for LEAK-  
 628 respiration) and is fully coupled to phosphorylation with a maximum mechanistic stoichiometry  
 629 (**Fig. 4**).

630 **LEAK-state (Fig. 5A)**: The LEAK-state is defined as a state of mitochondrial respiration  
 631 when O<sub>2</sub> flux mainly compensates for ion leaks in the absence of ATP synthesis, at kinetically-  
 632 saturating concentrations of O<sub>2</sub> and respiratory fuel substrates. LEAK-respiration is measured  
 633 to obtain an estimate of *intrinsic uncoupling* without addition of an experimental uncoupler: (1)



634 in the absence of adenylates; (2)  
 635 after depletion of ADP at a  
 636 maximum ATP/ADP ratio; or (3)  
 637 after inhibition of the  
 638 phosphorylation-pathway by  
 639 inhibitors of F-ATPase—such as  
 640 oligomycin, or of adenine  
 641 nucleotide translocase—such as  
 642 carboxyatractyloside.

643 Adjustment of the nominal  
 644 concentration of these inhibitors  
 645 to the density of biological  
 646 sample applied can minimize or  
 647 avoid inhibitory side-effects  
 648 exerted on ET-capacity or even  
 649 some dyscoupling.

650 **Proton leak and**  
 651 **uncoupled respiration:** Proton  
 652 leak is a leak current of protons.  
 653 The intrinsic proton leak is the  
 654 *uncoupled* process in which  
 655 protons diffuse across the mtIM  
 656 in the dissipative direction of the  
 657 downhill protonmotive force  
 658 without coupling to  
 659 phosphorylation (Fig. 5A). The  
 660 proton leak flux depends non-  
 661 linearly on the protonmotive  
 662 force (Garlid *et al.* 1989;  
 663 Divakaruni and Brand 2011), it is  
 664 a property of the mtIM and may  
 665 be enhanced due to possible  
 666 contaminations by free fatty  
 667 acids. Inducible uncoupling  
 668 mediated by uncoupling protein  
 669 1 (UCP1) is physiologically  
 670 controlled, *e.g.*, in brown  
 671 adipose tissue. UCP1 is a  
 672 member of the mitochondrial  
 673 carrier family which is involved  
 674 in the translocation of protons  
 675 across the mtIM (Klingenberg  
 676 2017). Consequently, the short-  
 677 circuit diminishes the protonmotive force and stimulates electron transfer to O<sub>2</sub> and heat dissipation without phosphorylation of ADP.

679 **Cation cycling:** There can be other cation contributors to leak current including calcium and probably magnesium. Calcium current is balanced by mitochondrial Na<sup>+</sup>/Ca<sup>2+</sup> exchange, which is balanced by Na<sup>+</sup>/H<sup>+</sup> or K<sup>+</sup>/H<sup>+</sup> exchanges. This is another effective uncoupling mechanism different from proton leak.

683  
 684

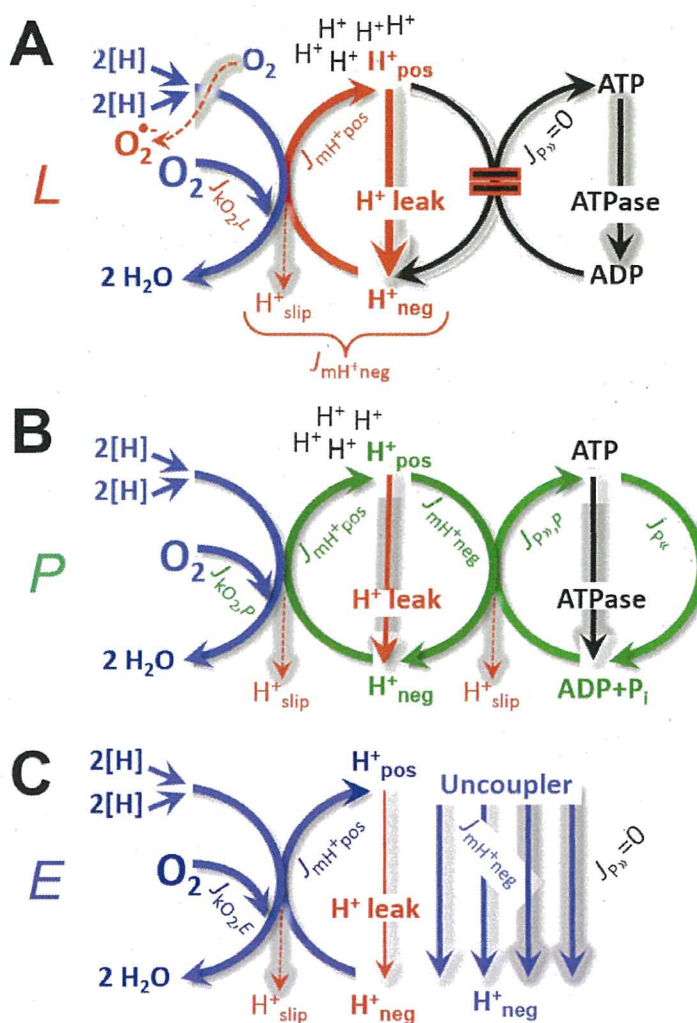


**Fig. 5. Respiratory coupling states. A: LEAK-state and rate, L:** Phosphorylation is arrested,  $J_{P_{\gg}} = 0$ , and catabolic O<sub>2</sub> flux,  $J_{kO_2,L}$ , is controlled mainly by the proton leak,  $J_{mH^+neg,L}$ , at maximum protonmotive force (Fig. 3). **B: OXPHOS-state and rate, P:** Phosphorylation,  $J_{P_{\gg}}$ , is stimulated by kinetically-saturating [ADP] and [P<sub>i</sub>], and is supported by a high protonmotive force. O<sub>2</sub> flux,  $J_{kO_2,P}$ , is well-coupled at a  $P_{\gg}/O_2$  ratio of  $J_{P_{\gg},P}/J_{O_2,P}$ . **C: ET-state and rate, E:** Noncoupled respiration,  $J_{kO_2,E}$ , is maximum at optimum exogenous uncoupler concentration and phosphorylation is zero,  $J_{P_{\gg}} = 0$ . See also Fig. 2.



685 **Table 2. Terms on respiratory coupling and uncoupling.**

Term	$J_{kO_2}$	$P \gg O_2$	Note	
acoupled		0	electron transfer in mitochondrial fragments without vectorial proton translocation ( <b>Fig. 3</b> )	
intrinsic, no protonophore added	$\left\{ \begin{array}{l} \text{uncoupled} \\ \text{proton leak-uncoupled} \\ \text{decoupled} \\ \text{loosely coupled} \\ \text{dyscoupled} \\ \text{inducibly uncoupled} \end{array} \right.$	$L$	0	non-phosphorylating LEAK-respiration ( <b>Fig. 5A</b> )
			0	component of $L$ , $H^+$ diffusion across the mtIM ( <b>Fig. 3</b> )
			0	component of $L$ , proton slip ( <b>Fig. 3</b> )
			0	component of $L$ , lower coupling due to superoxide formation and bypass of proton pumps ( <b>Fig. 3</b> )
			0	pathologically, toxicologically, environmentally increased uncoupling, mitochondrial dysfunction
			0	by UCP1 or cation ( <i>e.g.</i> , $Ca^{2+}$ ) cycling ( <b>Fig. 3</b> )
noncoupled	$E$	0	non-phosphorylating respiration stimulated to maximum flux at optimum exogenous uncoupler concentration ( <b>Fig. 5C</b> )	
well-coupled	$P$	high	phosphorylating respiration with an intrinsic LEAK component ( <b>Fig. 5B</b> )	
fully coupled	$P - L$	max.	OXPHOS-capacity corrected for LEAK-respiration ( <b>Fig. 4</b> )	

686

687

688

689

690

691

692

693

694

695

696

697

698

699

700

701

702

703

704

705

706

707

708

709

710

711

**Proton slip and decoupled respiration:** Proton slip is the *decoupled* process in which protons are only partially translocated by a proton pump of the ET-pathways and slip back to the original compartment. The proton leak is the dominant contributor to the overall leak current in mammalian mitochondria incubated under physiological conditions at 37 °C, whereas proton slip is increased at lower experimental temperature (Canton *et al.* 1995). Proton slip can also happen in association with the F-ATPase, in which the proton slips downhill across the pump to the matrix without contributing to ATP synthesis. In each case, proton slip is a property of the proton pump and increases with the pump turnover rate.

**Electron leak and loosely coupled respiration:** Superoxide production by the ETS leads to a bypass of proton pumps and correspondingly lower  $P \gg O_2$  ratio. This depends on the actual site of electron leak and the scavenging of hydrogen peroxide by cytochrome *c*, whereby electrons may re-enter the ETS with proton translocation by CIV.

**Loss of compartmental integrity and acoupled respiration:** Electron transfer and catabolic  $O_2$  flux proceed without compartmental proton translocation in disrupted mitochondrial fragments. Such fragments form during mitochondrial isolation, and may not fully fuse to re-establish structurally intact mitochondria. Loss of mtIM integrity, therefore, is the cause of acoupled respiration, which is a nonvectorial dissipative process without control by the protonmotive force.

**Dyscoupled respiration:** Mitochondrial injuries may lead to *dyscoupling* as a pathological or toxicological cause of *uncoupled* respiration. Dyscoupling may involve any type of uncoupling mechanism, *e.g.*, opening the permeability transition pore. Dyscoupled respiration is distinguished from the experimentally induced *noncoupled* respiration in the ET-state (**Fig. 3**).

**OXPHOS-state (Fig. 5B):** The OXPHOS-state is defined as the respiratory state with kinetically-saturating concentrations of  $O_2$ , respiratory and phosphorylation substrates, and

712 absence of exogenous uncoupler, which provides an estimate of the maximal respiratory  
 713 capacity in the OXPHOS-state for any given ET-pathway state. Respiratory capacities at  
 714 kinetically-saturating substrate concentrations provide reference values or upper limits of  
 715 performance, aiming at the generation of data sets for comparative purposes. Physiological  
 716 activities and effects of substrate kinetics can be evaluated relative to the OXPHOS-capacity.

717 As discussed previously, 0.2 mM ADP does not fully saturate flux in isolated  
 718 mitochondria (Gnaiger 2001; Puchowicz *et al.* 2004); greater ADP concentration is required,  
 719 particularly in permeabilized muscle fibres and cardiomyocytes, to overcome limitations by  
 720 intracellular diffusion and by the reduced conductance of the mtOM (Jepihhina *et al.* 2011,  
 721 Illaste *et al.* 2012, Simson *et al.* 2016), either through interaction with tubulin (Rostovtseva *et*  
 722 *al.* 2008) or other intracellular structures (Birkedal *et al.* 2014). In permeabilized muscle fibre  
 723 bundles of high respiratory capacity, the apparent  $K_m$  for ADP increases up to 0.5 mM (Saks *et*  
 724 *al.* 1998), consistent with experimental evidence that >90% saturation is reached only at >5  
 725 mM ADP (Pesta and Gnaiger 2012). Similar ADP concentrations are also required for accurate  
 726 determination of OXPHOS-capacity in human clinical cancer samples and permeabilized cells  
 727 (Klepinin *et al.* 2016; Koit *et al.* 2017). Whereas 2.5 to 5 mM ADP is sufficient to obtain the  
 728 actual OXPHOS-capacity in many types of permeabilized tissue and cell preparations,  
 729 experimental validation is required in each specific case.

730 **Electron transfer-state (Fig. 5C):** The ET-state is defined as the *noncoupled* state with  
 731 kinetically-saturating concentrations of O<sub>2</sub>, respiratory substrate and optimum *exogenous*  
 732 uncoupler concentration for maximum O<sub>2</sub> flux, as an estimate of ET-capacity. Inhibition of  
 733 respiration is observed at higher than optimum uncoupler concentrations. As a consequence of  
 734 the nearly collapsed protonmotive force, the driving force is insufficient for phosphorylation,  
 735 and  $J_{P_s} = 0$ .

736 **ROX state and Rox:** Besides the three fundamental coupling states of mitochondrial  
 737 preparations, the state of residual O<sub>2</sub> consumption, ROX, is relevant to assess respiratory  
 738 function. ROX is not a coupling state. The rate of residual oxygen consumption, *Rox*, is defined  
 739 as O<sub>2</sub> consumption due to oxidative side reactions remaining after inhibition of ET—with  
 740 rotenone, malonic acid and antimycin A. Cyanide and azide inhibit CIV and several peroxidases  
 741 involved in *Rox*. ROX represents a baseline that is used to correct mitochondrial respiration in  
 742 defined coupling states. *Rox* is not necessarily equivalent to non-mitochondrial respiration,  
 743 considering O<sub>2</sub>-consuming reactions in mitochondria not related to ET—such as O<sub>2</sub>  
 744 consumption in reactions catalyzed by monoamine oxidases (type A and B), monooxygenases  
 745 (cytochrome P450 monooxygenases), dioxygenase (sulfur dioxygenase and trimethyllysine  
 746 dioxygenase), and several hydroxylases. Mitochondrial preparations, especially those obtained  
 747 from liver, may be contaminated by peroxisomes. This fact makes the exact determination of  
 748 mitochondrial O<sub>2</sub> consumption and mitochondria-associated generation of reactive oxygen  
 749 species complicated (Schönfeld *et al.* 2009). The dependence of ROX-linked O<sub>2</sub> consumption  
 750 needs to be studied in detail together with non-ET enzyme activities, availability of specific  
 751 substrates, O<sub>2</sub> concentration, and electron leakage leading to the formation of reactive oxygen  
 752 species.

753

### 754 2.3. Classical terminology for isolated mitochondria

755 ‘When a code is familiar enough, it ceases appearing like a code; one forgets that there  
 756 is a decoding mechanism. The message is identical with its meaning’ (Hofstadter 1979).

757

758 Chance and Williams (1955; 1956) introduced five classical states of mitochondrial respiration  
 759 and cytochrome redox states. **Table 3** shows a protocol with isolated mitochondria in a closed  
 760 respirometric chamber, defining a sequence of respiratory states. States and rates are not  
 761 specifically distinguished in this nomenclature.

762



763  
764  
765**Table 3. Metabolic states of mitochondria (Chance and Williams, 1956; Table V).**

State	[O <sub>2</sub> ]	ADP level	Substrate level	Respiration rate	Rate-limiting substance
1	>0	low	low	slow	ADP
2	>0	high	~0	slow	substrate
3	>0	high	high	fast	respiratory chain
4	>0	low	high	slow	ADP
5	0	high	high	0	oxygen

766

767

768

769

**State 1** is obtained after addition of isolated mitochondria to air-saturated isoosmotic/isotonic respiration medium containing P<sub>i</sub>, but no fuel substrates and no adenylates, *i.e.*, AMP, ADP, ATP.

770

771

772

773

774

775

776

777

778

779

780

781

**State 2** is induced by addition of a 'high' concentration of ADP (typically 100 to 300 μM), which stimulates respiration transiently on the basis of endogenous fuel substrates and phosphorylates only a small portion of the added ADP. State 2 is then obtained at a low respiratory activity limited by exhausted endogenous fuel substrate availability (**Table 3**). If addition of specific inhibitors of respiratory complexes—such as rotenone—does not cause a further decline of O<sub>2</sub> flux, State 2 is equivalent to the ROX state (See below.). If inhibition is observed, undefined endogenous fuel substrates are a confounding factor of pathway control, contributing to the effect of subsequently externally added substrates and inhibitors. In contrast to the original protocol, an alternative sequence of titration steps is frequently applied, in which the alternative 'State 2' has an entirely different meaning, when this second state is induced by addition of fuel substrate without ADP (LEAK-state; in contrast to State 2 defined in **Table 1** as a ROX state), followed by addition of ADP.

782

783

784

785

786

787

788

789

790

791

792

793

794

**State 3** is the state stimulated by addition of fuel substrates while the ADP concentration is still high (**Table 3**) and supports coupled energy transformation through oxidative phosphorylation. 'High ADP' is a concentration of ADP specifically selected to allow the measurement of State 3 to State 4 transitions of isolated mitochondria in a closed respirometric chamber. Repeated ADP titration re-establishes State 3 at 'high ADP'. Starting at O<sub>2</sub> concentrations near air-saturation (ca. 200 μM O<sub>2</sub> at sea level and 37 °C), the total ADP concentration added must be low enough (typically 100 to 300 μM) to allow phosphorylation to ATP at a coupled O<sub>2</sub> flux that does not lead to O<sub>2</sub> depletion during the transition to State 4. In contrast, kinetically-saturating ADP concentrations usually are 10-fold higher than 'high ADP', *e.g.*, 2.5 mM in isolated mitochondria. The abbreviation State 3u is occasionally used in bioenergetics, to indicate the state of respiration after titration of an uncoupler, without sufficient emphasis on the fundamental difference between OXPHOS-capacity (*well-coupled* with an *endogenous* uncoupled component) and ET-capacity (*noncoupled*).

795

796

797

798

799

800

801

802

803

804

805

**State 4** is a LEAK-state that is obtained only if the mitochondrial preparation is intact and well-coupled. Depletion of ADP by phosphorylation to ATP leads to a decline of O<sub>2</sub> flux in the transition from State 3 to State 4. Under these conditions of State 4, a maximum protonmotive force and high ATP/ADP ratio are maintained. For calculation of P<sub>o</sub>/O<sub>2</sub> ratios the gradual decline of Y<sub>P<sub>o</sub>/O<sub>2</sub></sub> towards diminishing [ADP] at State 4 must be taken into account (Gnaiger 2001). State 4 respiration, L<sub>T</sub> (**Table 1**), reflects intrinsic proton leak and intrinsic ATP hydrolysis activity. O<sub>2</sub> flux in State 4 is an overestimation of LEAK-respiration if the contaminating ATP hydrolysis activity recycles some ATP to ADP, J<sub>P<sub>o</sub></sub>, which stimulates respiration coupled to phosphorylation, J<sub>P<sub>o</sub></sub> > 0. This can be tested by inhibition of the phosphorylation-pathway using oligomycin, ensuring that J<sub>P<sub>o</sub></sub> = 0 (State 4o). Alternatively, sequential ADP titrations re-establish State 3, followed by State 3 to State 4 transitions while

806 sufficient O<sub>2</sub> is available. Anoxia may be reached, however, before exhaustion of ADP (State  
807 5).

808 **State 5** is the state after exhaustion of O<sub>2</sub> in a closed respirometric chamber. Diffusion of  
809 O<sub>2</sub> from the surroundings into the aqueous solution may be a confounding factor preventing  
810 complete anoxia (Gnaiger 2001). Chance and Williams (1955) provide an alternative definition  
811 of State 5, which gives it the different meaning of ROX versus anoxia: ‘State 5 may be obtained  
812 by antimycin A treatment or by anaerobiosis’.

813 In **Table 3**, only States 3 and 4 (and ‘State 2’ in the alternative protocol: addition of fuel  
814 substrates without ADP; not included in the table) are coupling control states, with the  
815 restriction that O<sub>2</sub> flux in State 3 may be limited kinetically by non-saturating ADP  
816 concentrations (**Table 1**).

817

818

### 819 3. Normalization: fluxes and flows

820

#### 821 3.1. Normalization: system or sample

822

823 The term *rate* is not sufficiently defined to be useful for reporting data (**Fig. 6**). The  
824 inconsistency of the meanings of rate becomes fully apparent when considering Galileo  
825 Galilei’s famous principle, that ‘bodies of different weight all fall at the same rate (have a  
826 constant acceleration)’ (Coopersmith 2010).

827

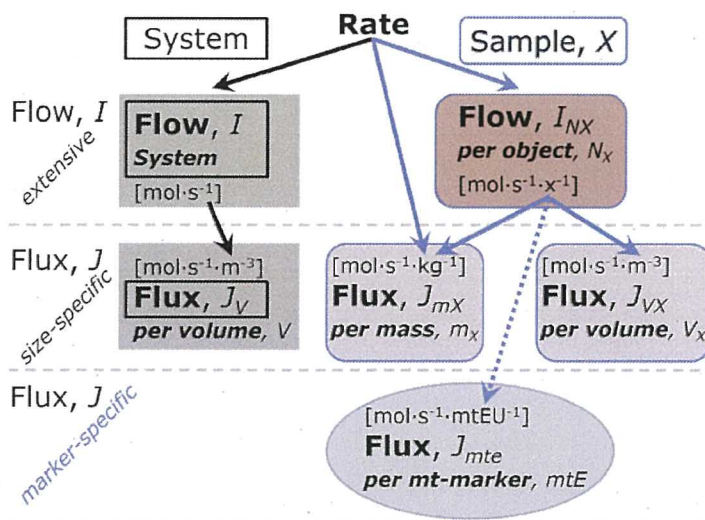
828 **Fig. 6. Different meanings of rate may lead to confusion, if the normalization is not**  
829 **sufficiently specified.** Results are frequently expressed as mass-  
830 specific *flux*,  $J_{mX}$ , per mg protein, dry or wet weight (mass). Cell  
831 volume,  $V_{\text{cell}}$ , may be used for normalization (volume-specific  
832 flux,  $J_{V\text{cell}}$ ), which must be clearly distinguished from flow per cell,  
833  $I_{N\text{cell}}$ , or flux,  $J_V$ , expressed for methodological reasons per  
834 volume of the measurement system. For details see **Table 4**.

843

844 **Flow per system,  $I$ :** In a generalization of electrical terms, flow as an extensive quantity  
845 ( $I$ ; per system) is distinguished from flux as a size-specific quantity ( $J$ ; per system size) (**Fig.**  
846 **6**). Electric current is flow,  $I_{\text{el}}$  [ $\text{A} \equiv \text{C} \cdot \text{s}^{-1}$ ] per system (extensive quantity). When dividing this  
847 extensive quantity by system size (cross-sectional area of a ‘wire’), a size-specific quantity is  
848 obtained, which is flux (current density),  $J_{\text{el}}$  [ $\text{A} \cdot \text{m}^{-2} = \text{C} \cdot \text{s}^{-1} \cdot \text{m}^{-2}$ ].

849 **Extensive quantities:** An extensive quantity increases proportionally with system size.  
850 The magnitude of an extensive quantity is completely additive for non-interacting  
851 subsystems—such as mass or flow expressed per defined system. The magnitude of these  
852 quantities depends on the extent or size of the system (Cohen *et al.* 2008).

853 **Size-specific quantities:** ‘The adjective *specific* before the name of an extensive quantity  
854 is often used to mean *divided by mass*’ (Cohen *et al.* 2008). In this system-paradigm, mass-  
855 specific flux is flow divided by mass of the *system* (the total mass of everything within the  
856 measuring chamber or reactor). A mass-specific quantity is independent of the extent of non-  
857 interacting homogenous subsystems. Tissue-specific quantities (related to the *sample* in





858 contrast to the *system*) are of fundamental interest in comparative mitochondrial physiology,  
 859 where *specific* refers to the *type of the sample* rather than *mass of the system*. The term *specific*,  
 860 therefore, must be clarified; *sample-specific*, e.g., muscle mass-specific normalization, is  
 861 distinguished from *system-specific* quantities (mass or volume; **Fig. 6**).  
 862

---

### 863 **Box 2: Metabolic fluxes and flows: vectorial and scalar**

864

865 Fluxes are *vectors*, if they have *spatial* geometric direction in addition to magnitude.  
 866 Electric charge per unit time is electric flow or current,  $I_{el} = dQ_{el} \cdot dt^{-1}$  [A]. When expressed per  
 867 unit cross-sectional area,  $A$  [ $m^2$ ], a vector flux is obtained, which is current density or surface-  
 868 density of flow) perpendicular to the direction of flux,  $J_{el} = I_{el} \cdot A^{-1}$  [ $A \cdot m^{-2}$ ] (Cohen et al. 2008).  
 869 For all transformations *flows*,  $I_{tr}$ , are defined as extensive quantities. Vector and scalar *fluxes*  
 870 are obtained as  $J_{tr} = I_{tr} \cdot A^{-1}$  [ $mol \cdot s^{-1} \cdot m^{-2}$ ] and  $J_{tr} = I_{tr} \cdot V^{-1}$  [ $mol \cdot s^{-1} \cdot m^{-3}$ ], expressing flux as an area-  
 871 specific vector or volume-specific vectorial or scalar quantity, respectively (Gnaiger 1993b).

872 We suggest to define: (1) *vectorial* fluxes, which are translocations as functions of  
 873 *gradients* with direction in geometric space in continuous systems; (2) *vectorial* fluxes, which  
 874 describe translocations in discontinuous systems and are restricted to information on  
 875 *compartmental differences* (**Fig. 2**, transmembrane proton flux); and (3) *scalar* fluxes, which  
 876 are transformations in a *homogenous* system (**Fig. 2**, catabolic  $O_2$  flux,  $J_{kO_2}$ ).

877 Vectorial transmembrane proton fluxes,  $J_{mH^+pos}$  and  $J_{mH^+neg}$ , are analyzed in a  
 878 heterogenous compartmental system as a quantity with *directional* but not *spatial* information.  
 879 Translocation of protons across the mtIM has a defined direction, either from the negative  
 880 compartment (matrix space; negative, neg-compartment) to the positive compartment (inter-  
 881 membrane space; positive, pos-compartment) or *vice versa* (**Fig. 2**). The arrows defining the  
 882 direction of the translocation between the two compartments may point upwards or downwards,  
 883 right or left, without any implication that these are actual directions in space. The pos-  
 884 compartment is neither above nor below the neg-compartment in a spatial sense, but can be  
 885 visualized arbitrarily in a figure in the upper position (**Fig. 2**). In general, the *compartmental*  
 886 *direction* of vectorial translocation from the neg-compartment to the pos-compartment is  
 887 defined by assigning the initial and final state as *ergodynamic compartments*,  $H^+_{neg} \rightarrow H^+_{pos}$  or  
 888  $0 = -1 H^+_{neg} + 1 H^+_{pos}$ , related to work (erg = work) that must be performed to lift the proton from  
 889 a lower to a higher electrochemical potential or from the lower to the higher ergodynamic  
 890 compartment (Gnaiger 1993b).

891 In analogy to *vectorial* translocation, the direction of a *scalar* chemical reaction,  $A \rightarrow B$   
 892 or  $0 = -1 A + 1 B$ , is defined by assigning substrates and products, A and B, as ergodynamic  
 893 compartments.  $O_2$  is defined as a substrate in respiratory  $O_2$  consumption, which together with  
 894 the fuel substrates comprises the substrate compartment of the catabolic reaction (**Fig. 2**).  
 895 Volume-specific scalar  $O_2$  flux is coupled to vectorial translocation, yielding the  $H^+_{pos}/O_2$  ratio  
 896 (**Fig. 1**).  
 897

898

---

### 899 3.2. Normalization for system-size: flux per chamber volume

900

901 **System-specific flux,  $J_{V,O_2}$ :** The experimental system (experimental chamber) is part of  
 902 the measurement apparatus, separated from the environment as an isolated, closed, open,  
 903 isothermal or non-isothermal system (**Table 4**). On another level, we distinguish between (1)  
 904 the *system* with volume  $V$  and mass  $m$  defined by the system boundaries, and (2) the *sample* or  
 905 *objects* with volume  $V_X$  and mass  $m_X$  which are enclosed in the experimental chamber (**Fig. 6**).  
 906 Metabolic  $O_2$  flow per object,  $I_{O_2/X}$ , increases as the mass of the object is increased. Sample  
 907 mass-specific  $O_2$  flux,  $J_{O_2/mX}$  should be independent of the mass of the sample studied in the  
 908 instrument chamber, but system volume-specific  $O_2$  flux,  $J_{V,O_2}$  (per volume of the instrument

that

909 chamber), should increase in direct proportion to the mass of the sample in the chamber.  
 910 Whereas  $J_{V,O_2}$  depends on mass-concentration of the sample in the chamber, it should be  
 911 independent of the chamber (system) volume at constant sample mass. There are practical  
 912 limitations to increase the mass-concentration of the sample in the chamber, when one is  
 913 concerned about crowding effects and instrumental time resolution.

914 When the reactor volume does not change during the reaction, which is typical for liquid  
 915 phase reactions, the volume-specific *flux of a chemical reaction*  $r$  is the time derivative of the  
 916 advancement of the reaction per unit volume,  $J_{V,rB} = d_r \zeta_B / dt \cdot V^{-1}$  [(mol·s<sup>-1</sup>)·L<sup>-1</sup>]. The *rate of*  
 917 *concentration change* is  $dc_B/dt$  [(mol·L<sup>-1</sup>)·s<sup>-1</sup>], where concentration is  $c_B = n_B/V$ . There is a  
 918 difference between (1)  $J_{V,O_2}$  [mol·s<sup>-1</sup>·L<sup>-1</sup>] and (2) rate of concentration change [mol·L<sup>-1</sup>·s<sup>-1</sup>].  
 919 These merge to a single expression only in closed systems. In open systems, external fluxes  
 920 (such as O<sub>2</sub> supply) are distinguished from internal transformations (catabolic flux, O<sub>2</sub>  
 921 consumption). In a closed system, external flows of all substances are zero and O<sub>2</sub> consumption  
 922 (internal flow of catabolic reactions  $k$ ),  $I_{kO_2}$  [pmol·s<sup>-1</sup>], causes a decline of the amount of O<sub>2</sub> in  
 923 the system,  $n_{O_2}$  [nmol]. Normalization of these quantities for the volume of the system,  $V$  [L  $\equiv$   
 924 dm<sup>3</sup>], yields volume-specific O<sub>2</sub> flux,  $J_{V,kO_2} = I_{kO_2}/V$  [nmol·s<sup>-1</sup>·L<sup>-1</sup>], and O<sub>2</sub> concentration, [O<sub>2</sub>]  
 925 or  $c_{O_2} = n_{O_2}/V$  [ $\mu$ mol·L<sup>-1</sup> =  $\mu$ M = nmol·mL<sup>-1</sup>]. Instrumental background O<sub>2</sub> flux is due to external  
 926 flux into a non-ideal closed respirometer; then total volume-specific flux has to be corrected for  
 927 instrumental background O<sub>2</sub> flux—O<sub>2</sub> diffusion into or out of the instrumental chamber.  $J_{V,kO_2}$   
 928 is relevant mainly for methodological reasons and should be compared with the accuracy of  
 929 instrumental resolution of background-corrected flux, *e.g.*,  $\pm 1$  nmol·s<sup>-1</sup>·L<sup>-1</sup> (Gnaiger 2001).  
 930 ‘Metabolic’ or catabolic indicates O<sub>2</sub> flux,  $J_{kO_2}$ , corrected for: (1) instrumental background O<sub>2</sub>  
 931 flux; (2) chemical background O<sub>2</sub> flux due to autoxidation of chemical components added to  
 932 the incubation medium; and (3)  $R_{ox}$  for O<sub>2</sub>-consuming side reactions unrelated to the catabolic  
 933 pathway  $k$ .

934

### 935 3.3. Normalization: per sample

936

937 The challenges of measuring mitochondrial respiratory flux are matched by those of  
 938 normalization. Application of common and defined units is required for direct transfer of  
 939 reported results into a database. The second [s] is the *SI* unit for the base quantity *time*. It is also  
 940 the standard time-unit used in solution chemical kinetics. A rate may be considered as the  
 941 numerator and normalization as the complementary denominator, which are tightly linked in  
 942 reporting the measurements in a format commensurate with the requirements of a database.  
 943 Normalization (**Table 4**) is guided by physicochemical principles, methodological  
 944 considerations, and conceptual strategies (**Fig. 7**).

945 **Sample concentration,  $C_{mX}$ :** Normalization for sample concentration is required to  
 946 report respiratory data. Considering a tissue or cells as the sample,  $X$ , the sample mass is  $m_X$   
 947 [mg], which is frequently measured as wet or dry weight,  $W_w$  or  $W_d$  [mg], or as amount of tissue  
 948 or cell protein,  $m_{\text{Protein}}$ . In the case of permeabilized tissues, cells, and homogenates, the sample  
 949 concentration,  $C_{mX} = m_X/V$  [g·L<sup>-1</sup> = mg·mL<sup>-1</sup>], is the mass of the subsample of tissue that is  
 950 transferred into the instrument chamber.

951 **Mass-specific flux,  $J_{O_2/mX}$ :** Mass-specific flux is obtained by expressing respiration per  
 952 mass of sample,  $m_X$  [mg].  $X$  is the type of sample—isolated mitochondria, tissue homogenate,  
 953 permeabilized fibres or cells. Volume-specific flux is divided by mass concentration of  $X$ ,  $J_{O_2/mX}$   
 954 =  $J_{V,O_2}/C_{mX}$ ; or flow per cell is divided by mass per cell,  $J_{O_2/mcell} = I_{O_2/cell}/M_{cell}$ . If mass-specific  
 955 O<sub>2</sub> flux is constant and independent of sample size (expressed as mass), then there is no  
 956 interaction between the subsystems. A 1.5 mg and a 3.0 mg muscle sample respire at identical  
 957 mass-specific flux. Mass-specific O<sub>2</sub> flux, however, may change with the mass of a tissue  
 958 sample, cells or isolated mitochondria in the measuring chamber, in which the nature of the  
 959 interaction becomes an issue. Therefore, cell density must be optimized, particularly in



960 experiments carried out in wells, considering the confluency of the cell monolayer or clumps  
961 of cells (Salabei *et al.* 2014).

962 **Number concentration,  $C_{NX}$ :**  $C_{NX}$  is the experimental *number concentration* of sample  
963  $X$ . In the case of cells or animals, *e.g.*, nematodes,  $C_{NX} = N_X/V [X \cdot L^{-1}]$ , where  $N_X$  is the number  
964 of cells or organisms in the chamber (**Table 4**).

965

966

967

**Table 4. Sample concentrations and normalization of flux.**

Expression	Symbol	Definition	Unit	Notes
<b>Sample</b>				
identity of sample	$X$	object: cell, tissue, animal, patient		
number of sample entities $X$	$N_X$	number of objects	x	
mass of sample $X$	$m_X$		kg	1
mass of object $X$	$M_X$	$M_X = m_X \cdot N_X^{-1}$	$kg \cdot x^{-1}$	1
<b>Mitochondria</b>				
Mitochondria	mt	$X = mt$		
amount of mt-elements	$mtE$	quantity of mt-marker	mtEU	
<b>Concentrations</b>				
object number concentration	$C_{NX}$	$C_{NX} = N_X \cdot V^{-1}$	$x \cdot m^{-3}$	2
sample mass concentration	$C_{mX}$	$C_{mX} = m_X \cdot V^{-1}$	$kg \cdot m^{-3}$	
mitochondrial concentration	$C_{mtE}$	$C_{mtE} = mtE \cdot V^{-1}$	$mtEU \cdot m^{-3}$	3
specific mitochondrial density	$D_{mtE}$	$D_{mtE} = mtE \cdot m_X^{-1}$	$mtEU \cdot kg^{-1}$	4
mitochondrial content, $mtE$ per object $X$	$mtE_X$	$mtE_X = mtE \cdot N_X^{-1}$	$mtEU \cdot x^{-1}$	5
<b>O<sub>2</sub> flow and flux</b>				
flow, system	$I_{O_2}$	internal flow	$mol \cdot s^{-1}$	6
volume-specific flux	$J_{V,O_2}$	$J_{V,O_2} = I_{O_2} \cdot V^{-1}$	$mol \cdot s^{-1} \cdot m^{-3}$	7
flow per object $X$	$I_{O_2/X}$	$I_{O_2/X} = J_{V,O_2} \cdot C_{NX}^{-1}$	$mol \cdot s^{-1} \cdot x^{-1}$	8
mass-specific flux	$J_{O_2/mX}$	$J_{O_2/mX} = J_{V,O_2} \cdot C_{mX}^{-1}$	$mol \cdot s^{-1} \cdot kg^{-1}$	9
mitochondria-specific flux	$J_{O_2/mtE}$	$J_{O_2/mtE} = J_{V,O_2} \cdot C_{mtE}^{-1}$	$mol \cdot s^{-1} \cdot mtEU^{-1}$	10

968

969

970

971

972

973

974

975

976

977

978

979

980

981

982

983

984

985

986

1 The SI prefix k is used for the SI base unit of mass (kg = 1,000 g). In praxis, various SI prefixes are used for convenience, to make numbers easily readable, *e.g.*, 1 mg tissue, cell or mitochondrial mass instead of 0.000001 kg.

2 In case sample  $X =$  cells, the object number concentration is  $C_{N_{cell}} = N_{cell} \cdot V^{-1}$ , and volume may be expressed in [ $dm^3 \equiv L$ ] or [ $cm^3 = mL$ ]. See **Table 5** for different object types.

3 mt-concentration is an experimental variable, dependent on sample concentration: (1)  $C_{mtE} = mtE \cdot V^{-1}$ ; (2)  $C_{mtE} = mtE_X \cdot C_{NX}$ ; (3)  $C_{mtE} = C_{mX} \cdot D_{mtE}$ .

4 If the amount of mitochondria,  $mtE$ , is expressed as mitochondrial mass, then  $D_{mtE}$  is the mass fraction of mitochondria in the sample. If  $mtE$  is expressed as mitochondrial volume,  $V_{mt}$ , and the mass of sample,  $m_X$ , is replaced by volume of sample,  $V_X$ , then  $D_{mtE}$  is the volume fraction of mitochondria in the sample.

5  $mtE_X = mtE \cdot N_X^{-1} = C_{mtE} \cdot C_{NX}^{-1}$ .

6 O<sub>2</sub> can be replaced by other chemicals B to study different reactions, *e.g.*, ATP, H<sub>2</sub>O<sub>2</sub>, or compartmental translocations, *e.g.*, Ca<sup>2+</sup>.

7  $I_{O_2}$  and  $V$  are defined per instrument chamber as a system of constant volume (and constant temperature), which may be closed or open.  $I_{O_2}$  is abbreviated for  $I_{r,O_2}$ , *i.e.*, the metabolic or internal O<sub>2</sub> flow of the chemical reaction  $r$  in which O<sub>2</sub> is consumed, hence the negative stoichiometric number,  $\nu_{O_2} = -1$ .  $I_{r,O_2} = d_r n_{O_2} / dt \cdot \nu_{O_2}^{-1}$ . If  $r$  includes all chemical reactions in which O<sub>2</sub> participates, then  $d_r n_{O_2} = dn_{O_2} - d_e n_{O_2}$ , where  $dn_{O_2}$  is the change in the amount of O<sub>2</sub> in the instrument chamber and  $d_e n_{O_2}$

- 987 is the amount of O<sub>2</sub> added externally to the system. At steady state, by definition  $dn_{O_2} = 0$ , hence  $d_r n_{O_2}$   
 988  $= -d_e n_{O_2}$ .  
 989 8  $J_{V,O_2}$  is an experimental variable, expressed per volume of the instrument chamber.  
 990 9  $I_{O_2,X}$  is a physiological variable, depending on the size of entity X.  
 991 10 There are many ways to normalize for a mitochondrial marker, that are used in different experimental  
 992 approaches: (1)  $J_{O_2/mtE} = J_{V,O_2} \cdot C_{mtE}^{-1}$ ; (2)  $J_{O_2/mtE} = J_{V,O_2} \cdot C_{mX}^{-1} \cdot D_{mtE}^{-1} = J_{O_2,mX} \cdot D_{mtE}^{-1}$ ; (3)  $J_{O_2/mtE} =$   
 993  $J_{V,O_2} \cdot C_{mX}^{-1} \cdot mtE_X^{-1} = I_{O_2,X} \cdot mtE_X^{-1}$ ; (4)  $J_{O_2/mtE} = I_{O_2} \cdot mtE^{-1}$ . The mt-elemental unit [mtEU] varies between  
 994 different mt-markers.  
 995  
 996

**Table 5. Sample types, X, abbreviations, and quantification.**

Identity of sample	X	$N_X$	Mass <sup>a</sup>	Volume	mt-Marker
mitochondrial preparation	mt-prep	[x]	[kg]	[m <sup>3</sup> ]	[mtEU]
isolated mitochondria	imt		$m_{mt}$	$V_{mt}$	$mtE$
tissue homogenate	thom		$m_{thom}$		$mtE_{thom}$
permeabilized tissue	pti		$m_{pti}$		$mtE_{pti}$
permeabilized fibre	pfi		$m_{pfi}$		$mtE_{pfi}$
permeabilized cell	pce	$N_{pce}$	$M_{pce}$	$V_{pce}$	$mtE_{pce}$
intact cell	ce	$N_{ce}$	$M_{ce}$	$V_{ce}$	$mtE_{ce}$
Organism	org	$N_{org}$	$M_{org}$	$V_{org}$	

997 <sup>a</sup> Instead of mass, frequently the wet weight or dry weight is stated,  $W_w$  or  $W_d$ .  
 998  $m_X$  is mass of the sample [kg],  $M_X$  is mass of the object [kg·x<sup>-1</sup>].  
 999

1000 **Flow per object,  $I_{O_2,X}$ :** A special case of normalization is encountered in respiratory  
 1001 studies with permeabilized (or intact) cells. If respiration is expressed per cell, the O<sub>2</sub> flow per  
 1002 measurement system is replaced by the O<sub>2</sub> flow per cell,  $I_{O_2/cell}$  (**Table 4**). O<sub>2</sub> flow can be  
 1003 calculated from volume-specific O<sub>2</sub> flux,  $J_{V,O_2}$  [nmol·s<sup>-1</sup>·L<sup>-1</sup>] (per  $V$  of the measurement chamber  
 1004 [L]), divided by the number concentration of cells,  $C_{Nce} = N_{ce}/V$  [cell·L<sup>-1</sup>], where  $N_{ce}$  is the  
 1005 number of cells in the chamber. Cellular O<sub>2</sub> flow can be compared between cells of identical  
 1006 size. To take into account changes and differences in cell size, normalization is required to  
 1007 obtain cell size-specific or mitochondrial marker-specific O<sub>2</sub> flux (Renner *et al.* 2003).

1008 The complexity changes when the sample is a whole organism studied as an experimental  
 1009 model. The scaling law in respiratory physiology reveals a strong interaction of O<sub>2</sub> flow and  
 1010 individual body mass of an organism, since *basal* metabolic rate (flow) does not increase  
 1011 linearly with body mass, whereas *maximum* mass-specific O<sub>2</sub> flux,  $\dot{V}_{O_2max}$  or  $\dot{V}_{O_2peak}$ , is  
 1012 approximately constant across a large range of individual body mass (Weibel and Hoppeler  
 1013 2005), with individuals, breeds, and species deviating substantially from this relationship.  
 1014  $\dot{V}_{O_2peak}$  of human endurance athletes is 60 to 80 mL O<sub>2</sub>·min<sup>-1</sup>·kg<sup>-1</sup> body mass, converted to  
 1015  $J_{O_2peak/M}$  of 45 to 60 nmol·s<sup>-1</sup>·g<sup>-1</sup> (Gnaiger 2014; **Table 6**).  
 1016

### 1017 3.4. Normalization for mitochondrial content

1018 Tissues can contain multiple cell populations that may have distinct mitochondrial  
 1019 subtypes. Mitochondria undergo dynamic fission and fusion cycles, and can exist in multiple  
 1020 stages and sizes <sup>that</sup> which may be altered by a range of factors. The isolation of mitochondria (often  
 1021 achieved through differential centrifugation) can therefore yield a subsample of the  
 1022 mitochondrial types present in a tissue, depending on isolation protocols utilized (*e.g.*,  
 1023 centrifugation speed). This possible bias should be taken into account when planning  
 1024 experiments using isolated mitochondria. Different sizes of mitochondria are enriched at  
 1025 specific centrifugation speeds, which is used for isolation of mitochondrial subpopulations.  
 1026

1027 Part of the mitochondrial content of a tissue is lost during preparation of isolated  
 1028 mitochondria. The fraction of mitochondria in the isolate is expressed as mitochondrial  
 1029 recovery. At a high mitochondrial recovery the sample of isolated mitochondria is more



1030 representative of the total mitochondrial population than in preparations characterized by low  
 1031 recovery. Determination of the mitochondrial recovery and yield is based on measurement of  
 1032 the concentration of a mitochondrial marker in the tissue homogenate,  $C_{mtE,thom}$ , which  
 1033 simultaneously provides information on the specific mitochondrial density in the sample.

1034 Normalization is a problematic subject; it is essential to consider the question of the study.  
 1035 If the study aims at comparing tissue performance—such as the effects of a treatment on a  
 1036 specific tissue, then normalization can be successful, using tissue mass or protein content, for  
 1037 example. However, if the aim is to find differences on mitochondrial function independent of  
 1038 mitochondrial density (Table 4), then normalization to a mitochondrial marker is imperative  
 1039 (Fig. 7). One cannot assume that quantitative changes in various markers—such as  
 1040 mitochondrial proteins—necessarily occur in parallel with one another. It should be established  
 1041 that the marker chosen is not selectively altered by the performed treatment. In conclusion, the  
 1042 normalization must reflect the question under investigation to reach a satisfying answer. On the  
 1043 other hand, the goal of comparing results across projects and institutions requires  
 1044 standardization on normalization for entry into a databank.

1045

<b>Flow, Performance</b>	=	<b>Element function</b>	x	<b>Element density</b>	x	<b>Size of object</b>
$\frac{\text{mol}\cdot\text{s}^{-1}}{x}$	=	$\frac{\text{mol}\cdot\text{s}^{-1}}{x_{mtE}}$		$\frac{x_{mtE}}{\text{kg}}$		$\frac{\text{kg}}{x}$

<b>A</b>	<b>Flow</b>	=	<b>mt-specific flux</b>	x	<b>mt-structure, functional elements</b>
	$I_{O_2/X}$	=	$J_{O_2/mtE}$		$mtE_X$
					$\frac{mtE_X}{M_X} \cdot M_X$

	$I_{O_2/X}$	=	$J_{O_2/mtE}$		$D_{mtE}$		$M_X$
	$\frac{I_{O_2/X}}{M_X}$	=	$\frac{I_{O_2/X}}{mtE_X}$		$\frac{mtE_X}{M_X}$		

<b>B</b>	<b>Flow</b>	=	<b>Object mass-specific flux</b>	x	<b>Mass of object</b>
	$I_{O_2/X}$	=	$J_{O_2/MX}$		$M_X$

1046

1047

1048 **Fig. 7. Structure-function analysis of performance of an organism, organ or tissue, or a**  
 1049 **cell (sample entity, X). O<sub>2</sub> flow,  $I_{O_2/X}$ , is the product of performance per functional element**  
 1050 **(element function, mitochondria-specific flux), element density (mitochondrial density,**  
 1051  **$D_{mtE}$ ), and size of entity X (mass,  $M_X$ ). (A) Structured analysis: performance is the product of**  
 1052 **mitochondrial function (mt-specific flux) and structure (functional elements;  $D_{mtE}$  times mass**  
 1053 **of X). (B) Unstructured analysis: performance is the product of entity mass-specific flux,  $J_{O_2/MX}$**   
 1054  **$= I_{O_2/X}/M_X = I_{O_2}/m_X$  [mol·s<sup>-1</sup>·kg<sup>-1</sup>] and size of entity, expressed as mass of X;  $M_X = m_X \cdot N_X^{-1}$**   
 1055 **[kg·x<sup>-1</sup>]. See Table 4 for further explanation of quantities and units. Modified from Gnaiger**  
 1056 **(2014).**

1057

1058

1059

1060

1061

1062

**Mitochondrial concentration,  $C_{mtE}$ , and mitochondrial markers:** Mitochondrial organelles comprise a dynamic cellular reticulum in various states of fusion and fission. Hence, the definition of an "amount" of mitochondria is often misconceived: mitochondria cannot be counted reliably as a number of occurring elements. Therefore, quantification of the "amount" of mitochondria depends on the measurement of chosen mitochondrial markers. 'Mitochondria are the structural and functional elemental units of cell respiration' (Gnaiger 2014). The